32nd URSI GASS, Montreal, 19-26 August 2017

Transmission-Line Model for a Non-linear and Dispersive Parity-Time (PT) Symmetric Structure

Sendy Phang*(1), Gabriele Gradoni(1,2), Ana Vukovic(2), Stephen C. Creagh(1), and Trevor M. Benson(2)
(1) School of Mathematical Sciences, University of Nottingham, UK, NG7 2RD
(2) George Green Institute for Electromagnetics Research, University of Nottingham, UK, NG7 2RD

Abstract

The established time domain Transmission-Line Modelling (TLM) numerical method is extended to include models of (i) saturable dispersive gain and (ii) non-linear dielectric material. The method is used to simulate a photonic memory device based on a nonlinear Parity-Time (PT) structure.

1. Introduction

In [1], Bender and Boetcher describe a new class of a non-Hermitian Hamiltonian quantum mechanics (QM), the so called Parity-Time (PT) symmetric QM, in which they show that a Hamiltonian which satisfies a combined Parity and Time symmetry may have a completely *real spectrum*. Although the concept of PT-symmetry QM has been established since 1998, the practical implementation as a quantum mechanical system has been found to be problematic. However, the concept has been actively pursued in the context of photonic structures [2-6]. The PT concept can be exploited in photonics where an *ideal* PT-symmetric system translates to a photonics structure with a judicious profile of complex refractive index, which requires the combination of both *gain* and *loss* [2-3]. In the context of modeling such devices, we found that most of the work published to date has considered a dispersionless gain/loss material property. In [2,4], we have demonstrated that dispersion impacts on the spectral properties of PT-symmetric structures such that PT-symmetric condition can only be achieved at a single frequency in comparison to the dispersionless case.

In this paper, we extend our TLM PT model to include both material dispersion and non-linearity and apply it to a one-dimensional (1D) Bragg grating structure that can operate as a memory device.

The paper is organized as follows; in section 2, a brief introduction to PT-symmetric structures in photonics and their main features is given. In section 3, the dispersive saturable gain/loss model and the non-linear polarization model which are implemented within the TLM method are described. In Section 4 the application of the extended TLM model to simulate a non-linear PT-Bragg grating as a memory device is demonstrated.

2. Parity-Time (PT) Symmetric Structure

PT-symmetric photonics structures in photonics requires a judicious profile of complex material refractive index as [2-3],

$$n(-\boldsymbol{x}) = n^*(\boldsymbol{x}), \quad \text{where} \quad n = n' + jn'' \qquad (1).$$

that is, the real part of the refractive index n' is an even function whilst the imaginary part of the refractive index n'' is an odd function in space, $\boldsymbol{x}$.

A PT-symmetric structure features some unique properties in that it may have a completely real spectrum, i.e. zero net-power amplification or dissipation, despite having both gain and loss in the system. However, there exists an exceptional point, defined for a certain system parameters such as gain/loss or coupling strength, and operation beyond this point leads to an unstable system, characterized by complex eigenvalues.

3. Transmission-line Model for Nonlinear and Dispersive Gain/loss Medium

Throughout this paper, the established TLM method is used as our time-domain numerical simulation method [7-12]. In this paper, we do not attempt to describe in detail the basic concepts of the TLM method itself and readers are referred to some excellent references [7,10]. The original TLM formulation, [7], is based on propagating voltage/current impulses on an interconnected mesh of transmission lines, which mimics electromagnetic field propagation in both time and space. In this paper, a more general TLM implementation of the TLM is used based on the bilinear $\mathcal{Z}$ -transformation of Maxwell's equations [10,11] as it offers greater flexibility in describing general material properties [10].

As an illustration of how to implement the material model within the TLM method, the simplest case of 1D TLM is considered with the governing equation for the TLM node as [10]:

$$2V_y^r \equiv V_4^i + V_5^i = 2V_y + g_eV_y + 2\left(\frac{1-\mathcal{Z}^{-1}}{1+\mathcal{Z}^{-1}}\right)p_{ey} \qquad (2).$$

In (2), $V_{4,5}^i$ denote the incoming voltage pulses from the left and right of the node; V_y and i_z denote the nodal voltages and current respectively; g_e denotes the normalized conductivity, which is described in detail in Sec 3.1, and

p_{ey} is the normalized dielectric polarization. These TLM parameters are related to the physical electromagnetic parameters by

$$E \leftrightarrow -\frac{V}{\Delta\ell}\ ;\ H \leftrightarrow -\frac{i}{\Delta\ell\,\eta_0};\sigma_e \leftrightarrow \frac{g_e}{\Delta\ell\eta_0}\ ;\ p_e = -\frac{P_e\Delta\ell}{\varepsilon_0}, \qquad (3).$$

where $\Delta\ell = \Delta t c_0$ denotes the mesh size parameter and c_0 is the speed of light in free-space. Due to limitations of space, the reader is referred to [10,11] for detail of how to acquire these equivalences. In (2), a non-magnetic material is assumed. Note in (2), z^{-1} is the time-delay operator. In the following subsection, corresponding material parameters and their implementation within TLM are described.

3.1 Dispersive and Saturable Gain/Loss Model

In this paper, a macroscopic model of saturable dispersive gain/loss reported in [13] is considered by which material gain/loss is modeled by the conductivity as

$$\sigma_e(I,\omega) = \mathcal{S}(I)\frac{\sigma_0}{2}\left[\frac{1}{1+j(\omega-\omega_\sigma)\tau}+\frac{1}{1+j(\omega+\omega_\sigma)\tau}\right] \qquad (4).$$

where ω_σ denotes the atomic transitional angular frequency, τ is the atomic relaxation time parameter and σ_0 is related to the conductivity peak values set by the pumping level at ω_σ. The saturation coefficient $\mathcal{S}(I)$ describes the non-linear nature arising as a consequence of the finite number of electrons available in the case of a strong incident signal and is typically modeled as

$$\mathcal{S}(I) = \frac{1}{1+(I/I_{\text{sat}})}. \qquad (5).$$

In the case of a small incident signal the saturation coefficient is typically negligible. Upon application of $\mathcal{Z}$-transformation and field-circuit equivalences, eq. (4) can also be expressed in TLM parameters as [14]

$$g_e(I,z) = \mathcal{S}(I)\ \left[\frac{K_3+z^{-1}K_4+z^{-2}K_5}{K_6+z^{-1}K_7+z^{-2}K_8}\right], \qquad (6).$$

where the constants are given by

$$\begin{gathered} K_1 = 1/\tau\ ;\ K_2 = 1+(\omega_\sigma\tau)^2/\tau^2 \\ K_3 = 2K_1\Delta t + K_1^2\Delta t^2\ ;\ K_4 = 2(K_1\Delta t)^2 \\ K_5 = -2K_1\Delta t + K_1^2\Delta t^2\ ;\ K_6 = 4+4K_1\Delta t + K_2\Delta t^2 \\ K_7 = -8+2K_2(\Delta t)^2\ ;\ K_8 = 4-4K_1\Delta t + K_2\Delta t^2. \end{gathered} \qquad (7).$$

Since any causal system can be described by a past event, it can be shown that

$$(1+z^{-1})g_e = g_{e0} + z^{-1}\bar{g}_e(z), \qquad (8).$$

where the constant $g_{e0}$and the causal response $\bar{g}_e(z)$ are given by

$$\begin{gathered} g_{e0} = g_s\left(\frac{K_3}{K_6}\right) \\ \bar{g}(z) = \frac{b_0+z^{-1}b_1+z^{-2}b_2}{1-z^{-1}(-a_1)-z^{-2}(-a_2)} \end{gathered} \qquad (9).$$

Equation (8) is now ready to be implemented within the TLM algorithm.

3.2 Duffing Model of Nonlinear Materials

The Duffing model for the non-linear dielectric polarization is described in this section. The Duffing model is a dispersive non-linear model and has been extensively analyzed and shown to be superior to the Kerr model of a non-linear material [9]. The dielectric polarization can be expressed as,

$$P_e = \underbrace{\chi_{eL}|E|}_{\text{linear}} + \underbrace{\chi_e^{(2)}\ |E|^2 + \chi_e^{(3)}|E|^3}_{\text{nonlinear}}. \qquad (10).$$

The Duffing model can be expressed as in terms of normalized dielectric polarization [14],

$$\frac{\partial^2 p_D}{\partial T^2} + K_{D1}\frac{\partial p_D}{\partial T} + K_{D2}p_D f_D(p_{ey}) = K_{D3}V_y, \qquad (11).$$

where the constants are given by

$$K_{D1} = 2\delta\Delta t\ ;\ K_{D2} = \omega_{0D}^2\Delta t^2\ ;K_{D3} = \Delta\chi_{e0}\omega_{0D}^2\Delta t^2, \qquad (12).$$

with $\Delta\chi_{e0}$, ω_{0D} and δ are the dielectric DC susceptibility, Duffing polarization (angular) resonant frequency and the damping constant respectively. The function $f_D(p_{ey})$ describes the nonlinear nature of the Duffing equation and is given by [14]

$$f_D(p_{ey}) = e^{\alpha|p_{ey}|}. \qquad (13).$$

Here α is the Duffing non-linear constant and is related to the physical Kerr nonlinearity n_2 by [14]:

$$\alpha = -\frac{(\chi_{e\infty}+\Delta\chi_{e0}+1)^2 n_2}{\varepsilon_0^2\eta_0(\chi_{e\infty}+\Delta\chi_{e0})^2\Delta\chi_{e0}}. \qquad (14).$$

By an application of the bilinear $\mathcal{Z}$-transform, (11) can be expressed as,

$$p_D K_{D4} + p_D K_{D2} f_D(p_{ey}) + z^{-1}S_{D1} = K_{D3}V_y, \qquad (15).$$

where

$$\begin{gathered} K_{D4} = 4+2K_{D1} \\ S_{D1} = p_D(-8+2K_{D2}f_D) - 2K_{D3}V_y + z^{-1}S_{D2} \\ S_{D2} = p_D(4-2K_{D1}+K_{D2}f_D) - K_{D3}V_y. \end{gathered} \qquad (16).$$

3.3 Implementation of the Digital Filter

Now, we implement both the dispersive gain/loss model and the Duffing non-linear model. Substituting (8) to (2), one finds:

$$K_{e2}V_y + 2p_{Dy} = 2V_y^r + z^{-1}S_{ey} \qquad (17).$$

where,

$$\begin{gathered} K_{e1} = -(2+g_{e1}-2\chi_{e\infty})\ ;\ K_{e2} = 2+g_{e0}+2\chi_{e\infty} \\ S_{ey} = 2V_y^r + K_{e1}V_y + S_{ec} + 2p_{Dy}\ ;\ S_{ec} - \bar{g}_e(z)V_y. \end{gathered} \qquad (18).$$

The equations (17) and (15) are two coupled equations with two unknown variables, V_y and p_{Dy}, which are now ready to be solved simultaneously by bisection or the Newton-Rhapson iterative method [15].

4. A Non-linear PT Memory Device

In this section, the dispersive and non-linear TLM method is applied to model a nonlinear PT symmetric Bragg grating structure for application as a memory device. The 1D Bragg grating is schematically shown in Fig. 1.

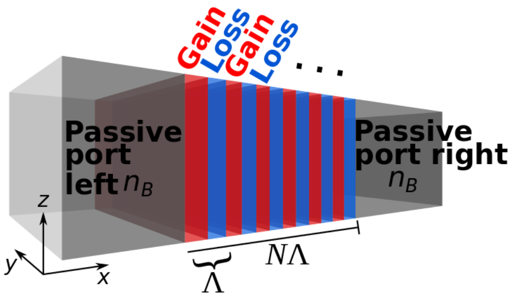

Figure 1. Schematic illustration of an N-period of non-linear PT-grating with a physical periodicity Λ.

Table 1. Frequency dependent material parameters of the nonlinear PT-grating [14]

Parameters	n_{lo}	n_{hi}
$\chi_{e\infty}$	2.5	2.8
$\Delta\chi_{e0}$	7.5	7.5
δ(rad/ps)	0.0923	0.0923
ω_{0D}(rad/ps)	4614.4	4614.4

The PT-grating considered has a Bragg resonance at $f_B = 336.85$ THz with $N = 200$ and embedded within a background material having a refractive index of $n_B = 3.626$. The refractive index profile for a single unit cell is given by,

$$n_G = \begin{cases} n_{hi} + n_2 I(x,t) - j\dfrac{c_0}{\omega}\alpha(\omega, I), x < \dfrac{\Lambda}{4} \\ n_{lo} + n_2 I(x,t) - j\dfrac{c_0}{\omega}\alpha(\omega, I), \dfrac{\Lambda}{4} < x < \dfrac{\Lambda}{2} \\ n_{lo} + n_2 I(x,t) + j\dfrac{c_0}{\omega}\alpha(\omega, I), \dfrac{\Lambda}{2} < x < \dfrac{3\Lambda}{4} \\ n_{hi} + n_2 I(x,t) + j\dfrac{c_0}{\omega}\alpha(\omega, I), \dfrac{3\Lambda}{4} < x < \Lambda \end{cases} \quad (19)$$

where n_{hi} and n_{lo} are frequency dependent complex high and low refractive index [14], (see table 1). For modeling purposes, the gain/loss material parameter is $\omega_\sigma = 2\pi f_B$, $\tau = 0.1$ ps and saturation intensity $I_{sat} = 5 \times 10^{13}\mathrm{W/m^2}$ [13,14]. The dispersive gain/loss α is modeled by the dispersive gain/loss material on which the peak gain/loss α_0 is related to the imaginary part of the refractive index by

$$\alpha_0 = \frac{\omega_\sigma}{c_0} n''(\omega_\sigma). \quad (20).$$

The transmittance of the non-linear PT-grating is plotted in Fig. 2 as the function of the input intensity, for different gain/loss parameters α, for the cases of excitation from the left T_L in Fig. 2(a) and right T_R in Fig. 2(b). In general, the transmittance of the PT-grating forms a hysteresis profile with the transmission from the right being different from transmission from the left, i.e. $T_L \neq T_R$. This inequality is one of the main features of the non-linear PT-grating which *violates the Lorentz reciprocity condition*. From Fig. 2, it can be seen that when the PT-grating is excited from the left side (hitting the gain section first), the presence of the gain/loss shifts the hysteresis to the left, such that the switching happens at a lower intensity compared to when the PT-grating is excited from the right side (hitting the lossy section first). The shift (from the passive case) is increased by increasing gain/loss in the material.

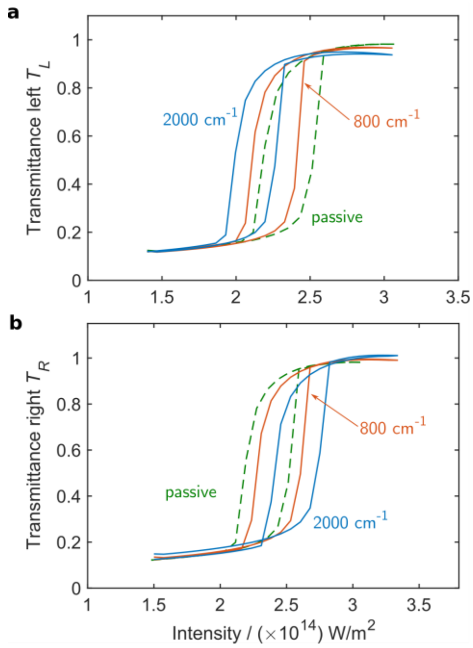

Figure 2. Hysteresis of the non-linear PT-grating for the case when excited from the left T_L (top part) and from the right T_R (bottom part). For different gain/loss parameter.

The bistable property of the non-linear PT-grating shown in Fig. 2 motivates the application of such a structure as a memory device with reduced input intensity. This application is demonstrated in Fig. 3 for the case of excitation from the left and the gain/loss parameter $\alpha = 2000\ \mathrm{cm^{-1}}$. Three different operations corresponding to write, read and reset are considered to emulate memory application. The read process is set with the intensity $I_{\mathrm{read}} = 2.2 \times 10^{14}\ \mathrm{W/m^2}$, writing intensity is $I_{\mathrm{write}} = 2.725 \times 10^{14}\ \mathrm{W/m^2}$ and reset intensity is $I_{\mathrm{reset}} = 1.5 \times 10^{14}\ \mathrm{W/m^2}$.

Figure 3(a) shows the input signal used in the TLM simulation, that is a repeated sequence of read, write, read, reset operations. The transmitted signal, in Fig 3(b), shows a distinct memory property; in the first read instance the transmitted intensity is low, as the PT-grating operated at the "0" state, after the write operation (set state to "1"), the following read operation gives a high transmittance for state “1”, the reset operation brings the memory state back to “0” and so forth.

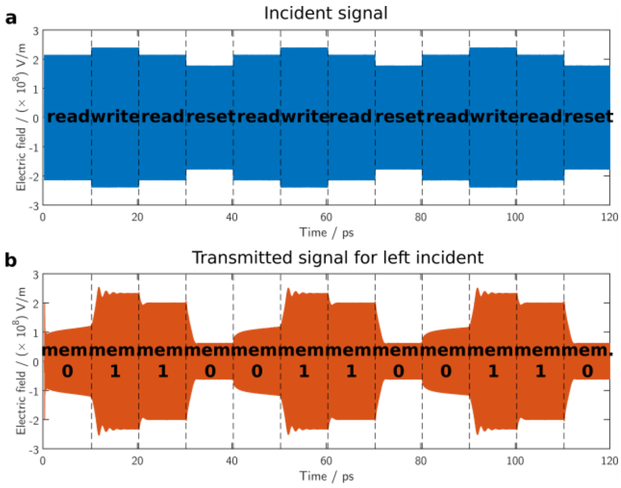

Figure 3. Demonstration of non-linear PT-grating as a memory device. (a) the input electric field and (b) the transmitted electric field for left incidence.

5. Summary

A dispersive-and-saturable gain/loss material model and a Duffing non-linear model for dielectric polarization are implemented within the TLM method. To demonstrate the application of the model, a non-linear Parity-Time (PT) symmetric Bragg grating is simulated. The results show a bistable operation that can be exploited in a memory device application. It is noted that the extended TLM method described in this paper can be used to model any arbitrary shape of PT-symmetric structure such as whispering gallery mode structures as in [2,3] or topological invariant PT-symmetric structures as in [3,6].

6. References

1. C. M. Bender, S. Boettcher, & P. N. Meisinger, “PT-symmetric quantum mechanics”. *Journal of Mathematical Physics*, 40(5), 2201-2229, 1999.
2. S. Phang, A. Vukovic, S. C. Creagh, T. M. Benson, P. D. Sewell, & G. Gradoni. “Parity-time symmetric coupled microresonators with a dispersive gain/loss”. *Optics express*, 23(9), 11493-11507, 2015.
3. ------. “Localized Single Frequency Lasing States in a Finite Parity-Time Symmetric Resonator Chain”. *Scientific Reports*, 6, 20499, 2016.
4. S. Phang, A. Vukovic, H. Susanto, T. M. Benson, & P. D. Sewell. “Impact of dispersive and saturable gain/loss on bistability of nonlinear parity–time Bragg gratings.” *Optics Letters*, 39(9), 2603-2606, 2014.
5. ------. “A versatile all-optical parity-time signal processing device using a Bragg grating induced using positive and negative Kerr-nonlinearity.” *Optical and Quantum Electronics*, 47(1), 37-47, 2015.
6. A. V. Poshakinskiy, A. N. Poddubny, L. Pilozzi, & E. L. Ivchenko. “Radiative topological states in resonant photonic crystals”. *PRL*, 112(10), 107403, 2014.
7. C. Christopoulos, The Transmission-Line Modeling Method; Oxford University Press: New York, 1995
8. P. Sewell, T.M. Benson, C. Christopoulos, D. W. P. Thomas, A. Vukovic, & J. G. Wykes. “Transmission-line modeling (TLM) based upon unstructured tetrahedral meshes.” *IEEE Microw. Theory Techn.*, 53(6), 1919-1928, 2005.
9. V. Janyani , A. Vukovic, J. D. Paul, P. D. Sewell, & T. M. Benson. “Time domain simulation in photonics: A comparison of nonlinear dispersive polarisation models.” *Opt. and quant. Elect.*, 37(1-3), 3-24, 2005.
10. J. Paul, C. Christopoulos, & D. W. Thomas. “Generalized material models in TLM. I. Materials with frequency-dependent properties.” *IEEE Trans. Antennas Propag.*, 47(10), 1528-1534, 1999.
11. ------. “Generalized material models in TLM-Part 3: materials with nonlinear properties.” *IEEE Trans. Antennas Propag*, 50(7), 997-1004, 2002.
12. X. Meng, P. Sewell, S. Phang, A. Vukovic, & T. M. Benson. Modeling curved carbon fiber composite (CFC) structures in the transmission-line modeling (TLM) method. *IEEE Trans. Electromagn. Compat.*, 57(3), 384-390, 2015.
13. S. C. Hagness, R. M. Joseph, & A. Taflove. “Subpicosecond electrodynamics of distributed Bragg reflector microlasers: Results from finite difference time domain simulations.” *Radio Science*, 31(4), 931-941, 1996.
14. S. Phang, A. Vukovic, H. Susanto, S. C. Creagh, P. Sewell, G. Gradoni, and T. M. Benson, “Theory and Numerical Modelling of Parity-Time Symmetric Structures in Photonics: Introduction and Grating Structures in One Dimension,” in Recent Trends in Computational Photonics, London, Springer Nature (2017).
15. Press, W. H., Teukolsky, S. A., Vetterling, W. T., & Flannery, B. P. (2007). Numerical recipes third edition: the art of scientific computing. Cambridge University Press, 32, 10013-2473.